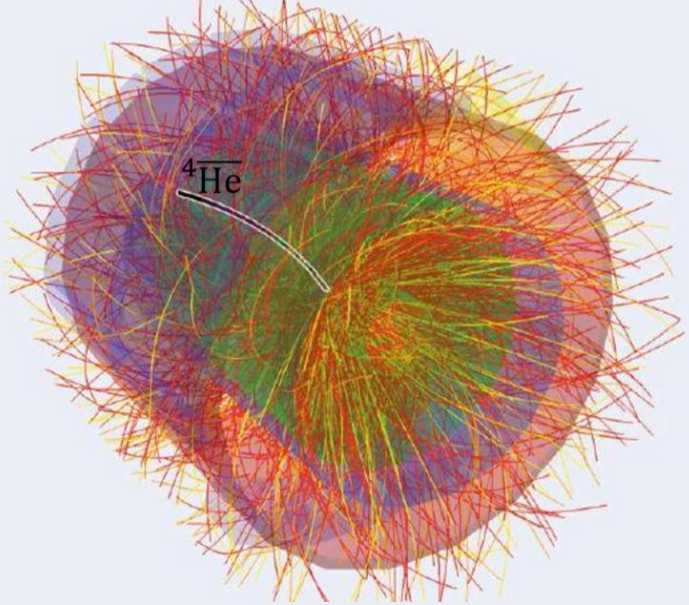

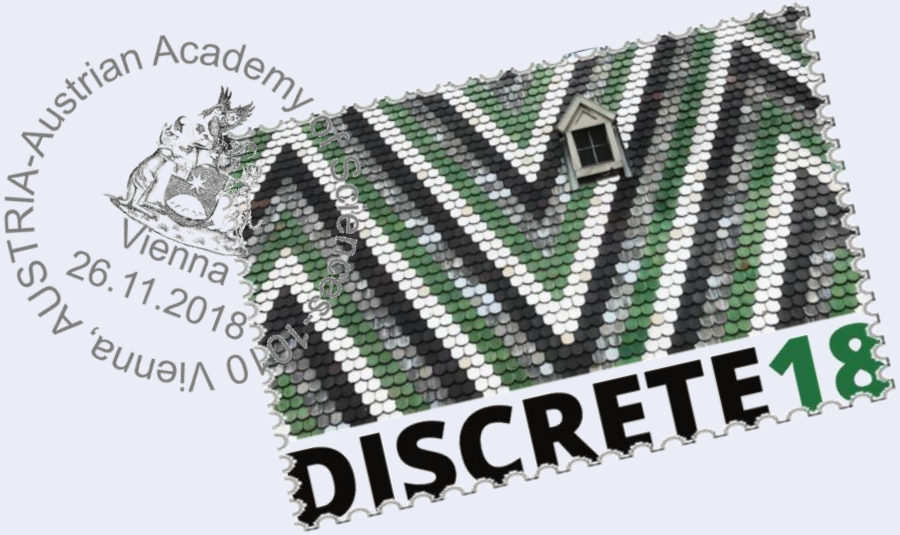

Precision measurement of the mass-to-charge difference between light nuclei and anti-nuclei with ALICE at the LHC

Francesco Noferini*

on behalf of the ALICE Collaboration

* INFN Bologna

Outline

- Motivations
- The ALICE experiment
- Analysis details
- Results
- Final remarks

Results published in Nature Phys. 11 (2015) 811
http://www.nature.com/nphys/journal/v11/n10/full/nphys3432.html

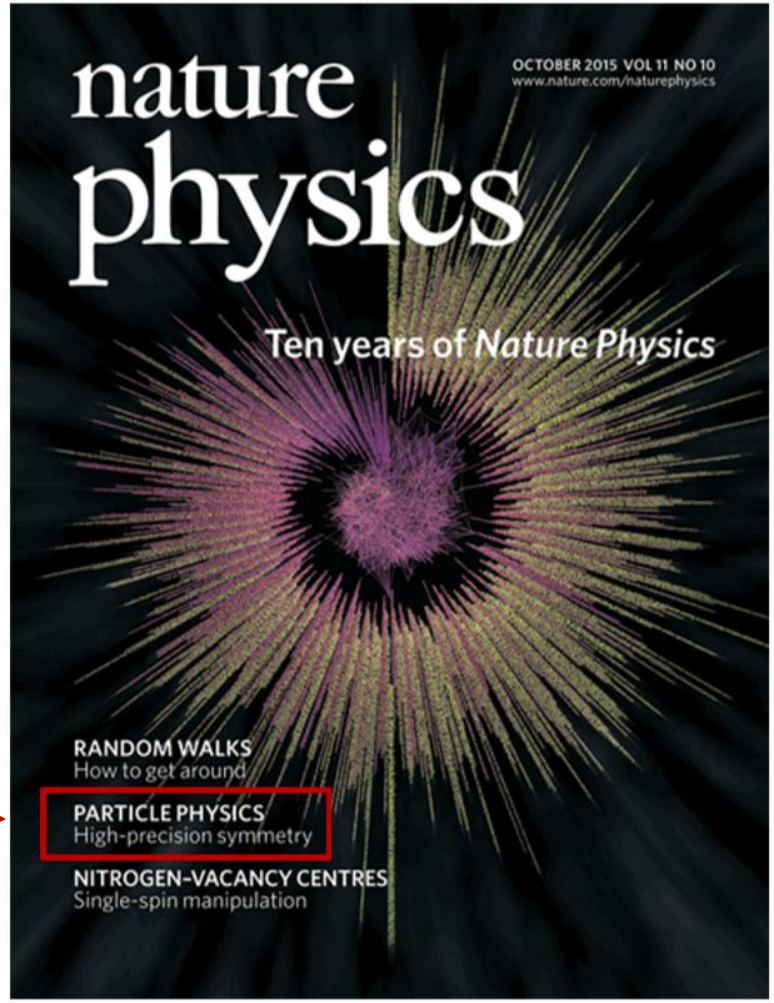

Motivations

The Standard Model predicts that in the primordial Universe there should have been equal amounts of matter and anti-matter. So far we are not able to reconcile expectations with observations → CPT violation?
Rev. Mod. Phys. 53 (1981) 141, Phys. Lett. B 725 (2013) 407

The CPT theorem demonstrates that CPT symmetry is guaranteed within a RQFT description of interactions constructed in a flat space-time (1), based on Lorentz invariance (2) and on the locality of the interactions (3).

If some of the conditions which back-up the CPT theorem are not satisfied, the symmetry is no longer guaranteed (see e.g. Phys. Rev. D 92 (2015) 056002). Many experiments are looking for possible CPT violation: mass, lifetime, charge, …

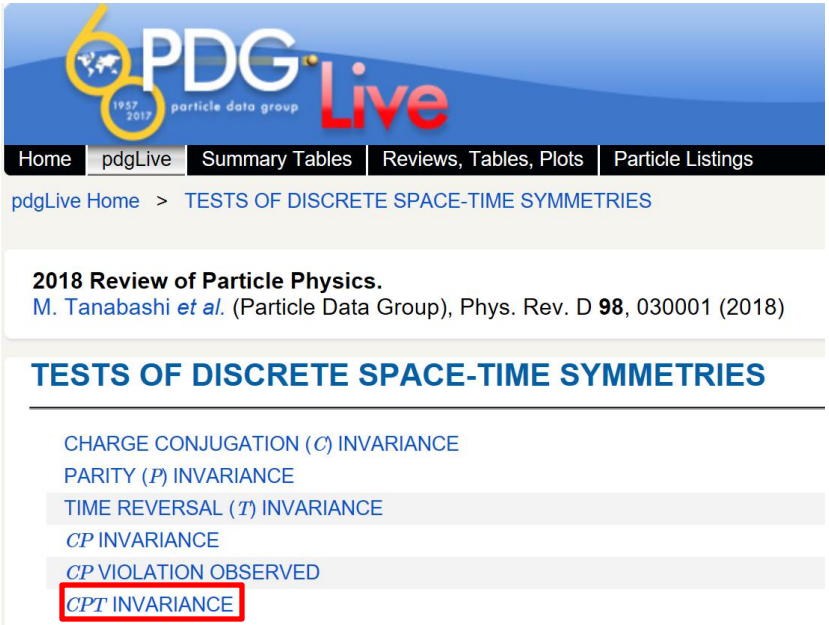

From (anti-)baryons to (anti-)nuclei

The extension of the measurement from (anti-)baryons to (anti-)nuclei allows one to probe any difference in the interactions between nucleons and anti-nucleons encoded in the (anti-)nuclei masses, a remnant of the underlying strong interaction among quarks and gluons not yet directly derived from quantum chromodynamics.

(anti)baryons → (anti)nuclei: binding energy ε_A

$$m_A = Zm_p + (A-Z)m_n - \varepsilon_A$$

$$m_{\bar{A}} = Zm_{\bar{p}} + (A-Z)m_{\bar{n}} - \varepsilon_{\bar{A}}$$

LHC as an (anti-)nuclei factory

Nucl. Phys. A971 (2018) 1

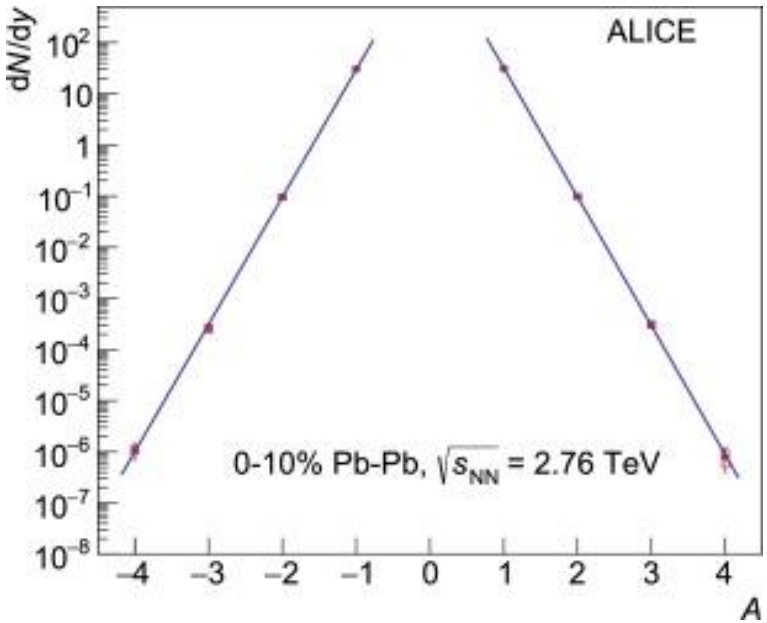

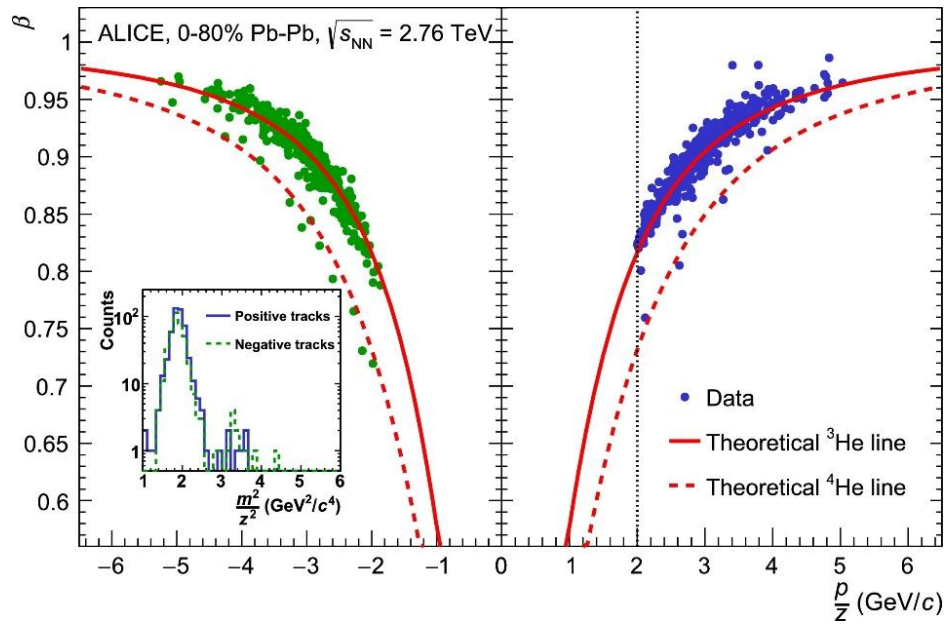

So far the heaviest anti-nucleus observed is the anti-alpha ($^4\overline{He}$). $^4\overline{He}$ was seen for the first time by the STAR Collaboration (Nature 473 (2011) 353) at RHIC and then observed also at the LHC by ALICE .

Anti-nuclei production in AA collisions

Double charged (anti-)nuclei (He and $\overline{He}$) are easier to be identified (see next slides)

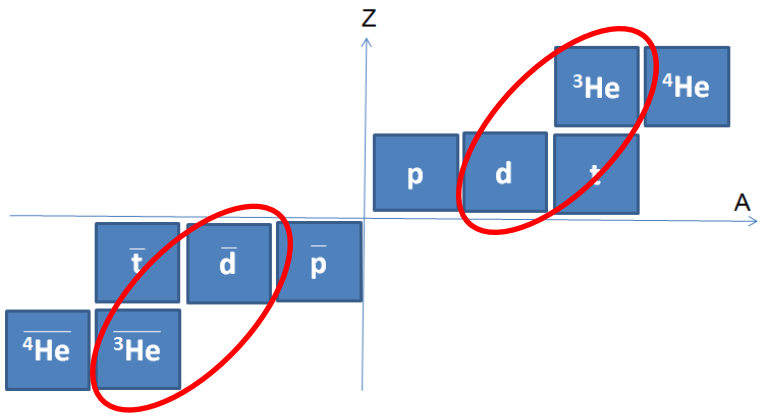

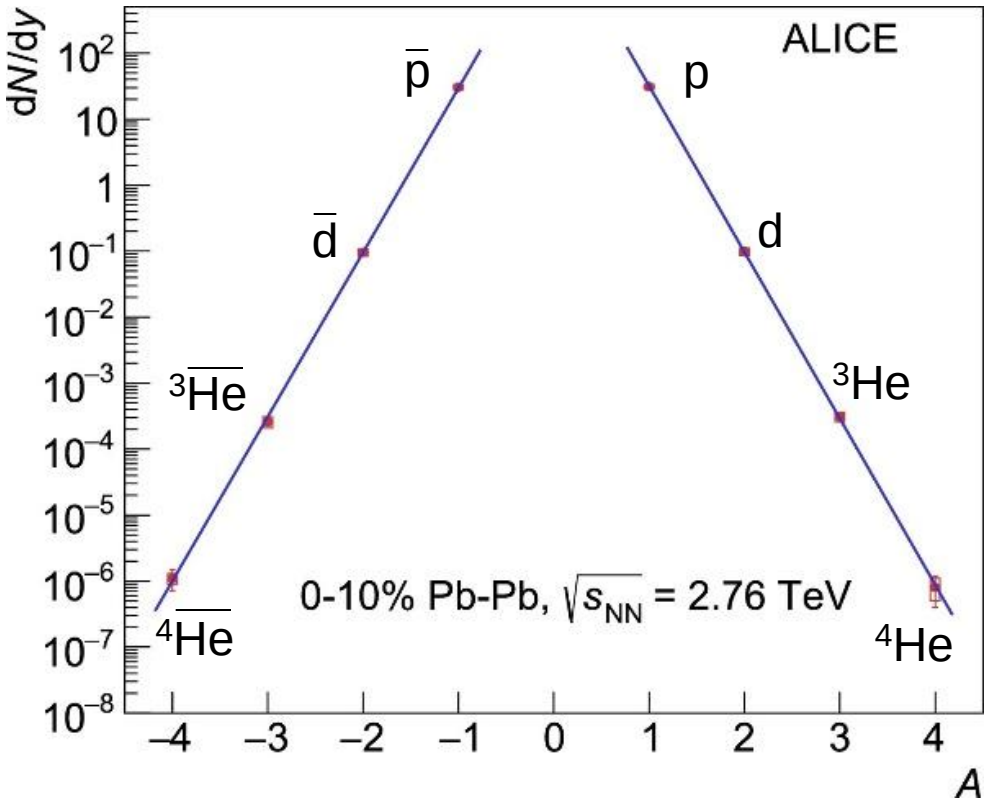

The penalty factor, namely the reduction of the yield by adding one nucleon, is approximately 300 extracted by fitting the light nuclei yields.

Analysis details

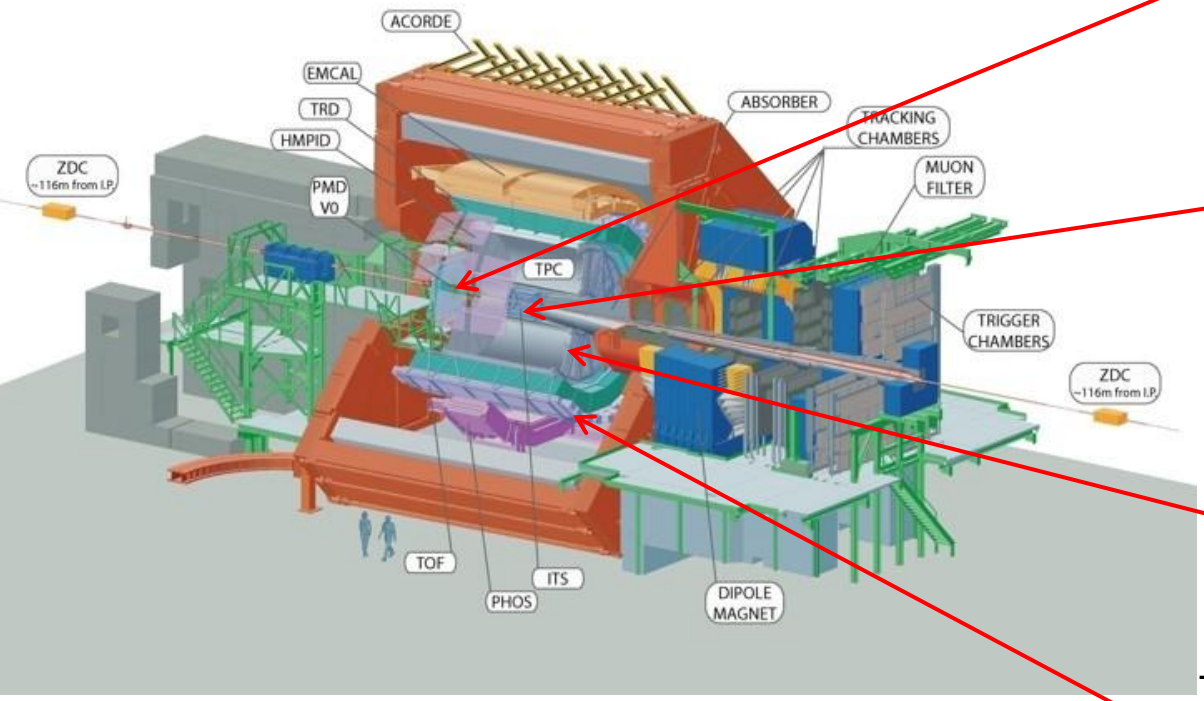

VZERO detector
Two forward scintillator arrays
($-3.7<\eta<-1.7$, $2.8<\eta<5.1$):
Triggering and beam-gas rejection

Inner Tracking System
(ITS)
($-0.8<\eta<0.8$)
Tracking + triggering

Time Projection Chamber
(TPC):
($-0.8<\eta<0.8$)
Tracking + particle identification(PID)

Time Of Flight (TOF):
($-0.8<\eta<0.8$)
Mass/Charge measurement

DATA sample:
Pb-Pb at $\sqrt{s_{NN}}$ = 2.76 TeV **(2011 data, 67M events)**
Trigger selection:
enriched in **central and semi-central collisions**

Particle identification with the TPC

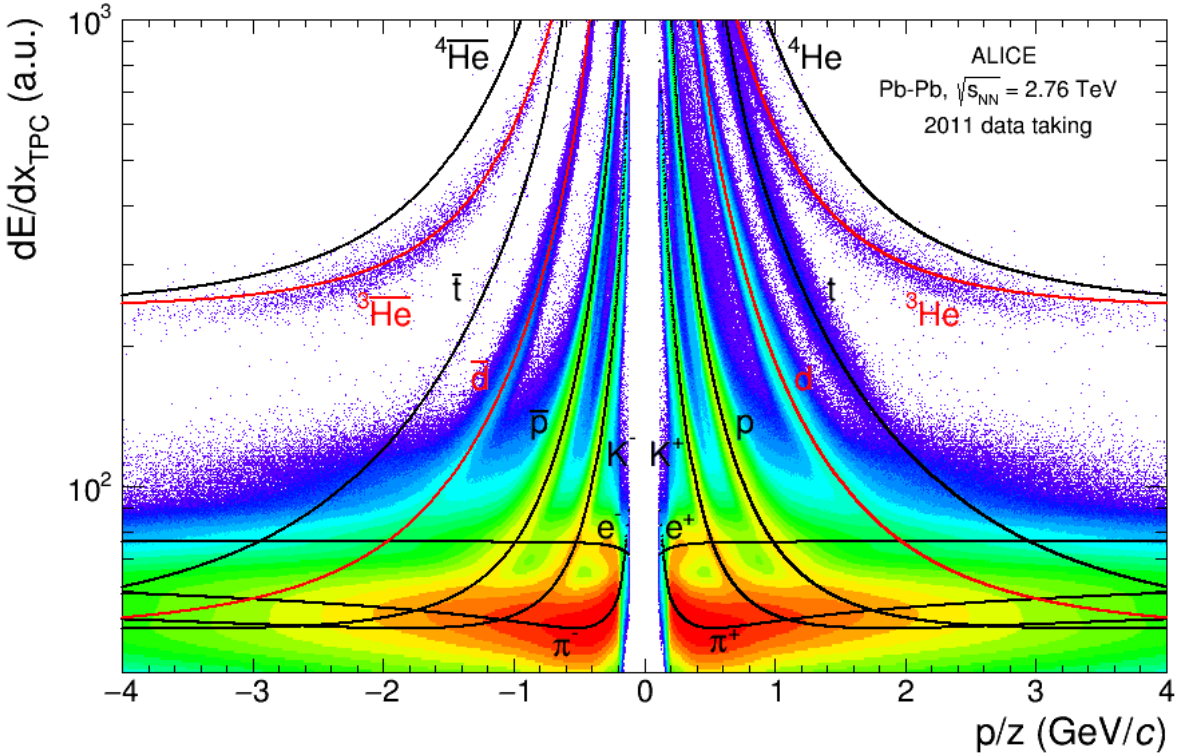

The TPC is able to identify (anti)deuteron up to *p/z* ~ 2 GeV/*c*.

For the (anti-)He case the larger charge (*Z*=2) determines a larger energy loss (even in the MIP region) allowing one to separate (anti-)He from hadrons in the full momentum region.

(anti-)^{3}He is a better candidate than (anti-)triton even if they have a similar mass → see also next slides.

Particle identification with the TOF

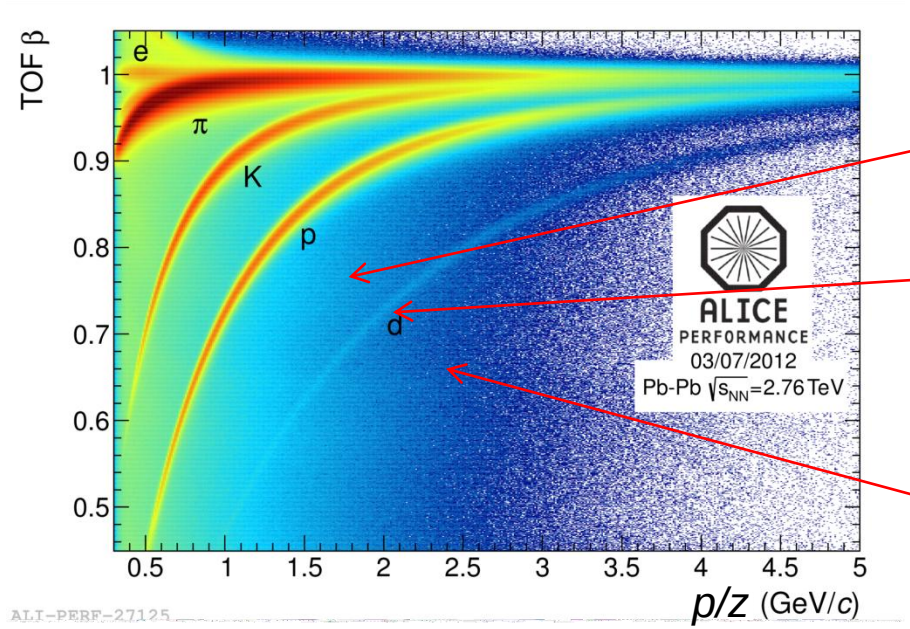

^{3}He is expected to be between p and d in the (β, *m/z)* plot.

^{4}He is expected to reach the TOF at the same time as a deuteron (because of the same m/z ratio)

The background dominates in case of triton

Light nuclei are well identified by TOF up to very high rigidities, thanks to a time resolution of 80 ps.

TPC track–TOF time mis-association is the bigger source of background (especially at low rigidities).

Particle identification with the TOF & TPC

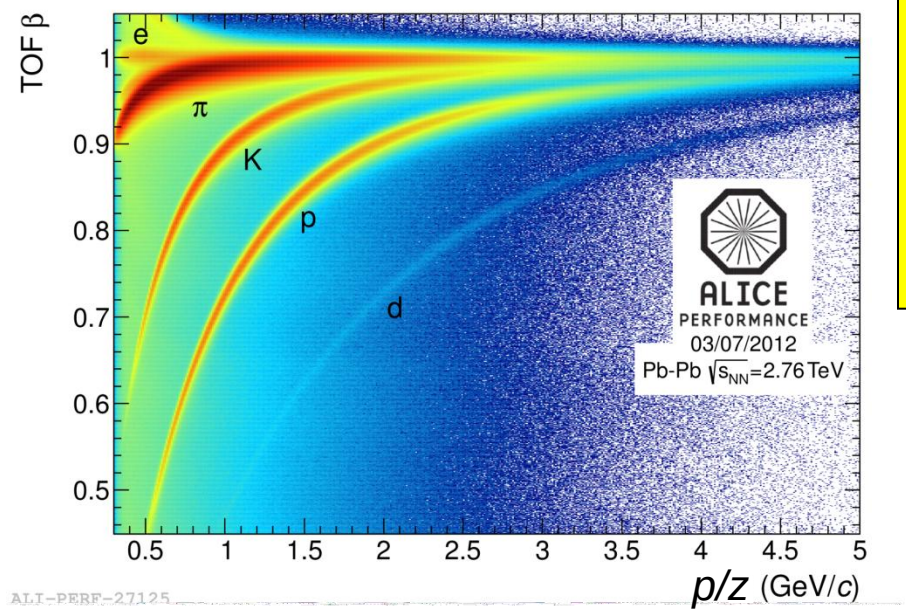

By combining TPC and TOF information the background around the TOF (anti-)He bands is removed (thanks to Z=2)

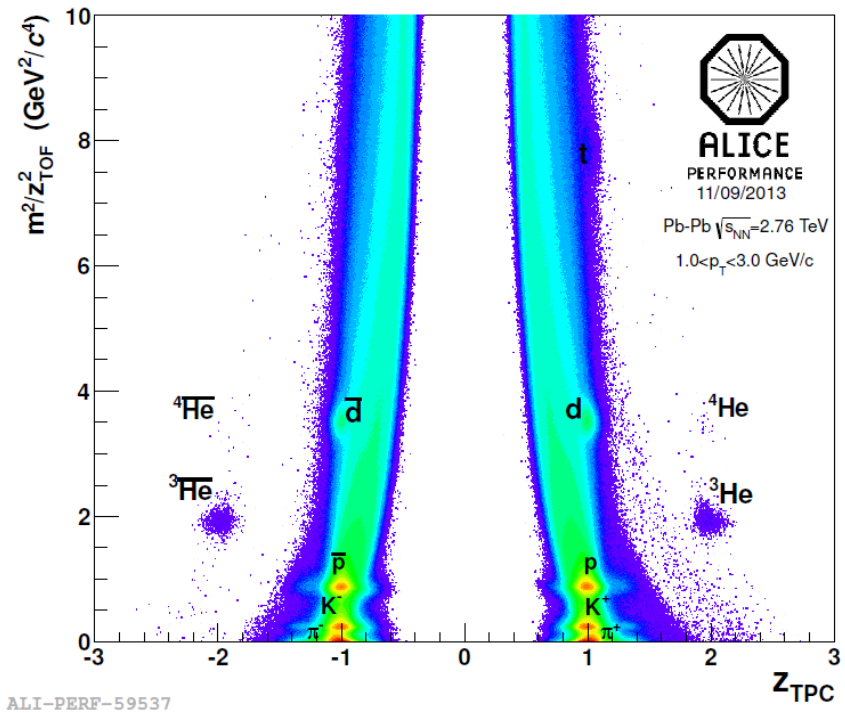

$$\mu^2_{TOF} = \left(\frac{m}{z}\right)^2_{TOF} = \left(\frac{p}{z}\right)^2 \left[\left(\frac{t_{TOF}}{L}\right)^2 - \frac{1}{c^2}\right]$$

$$z^2_{TPC} = \frac{(dE/dx)_{TPC}}{(dE/dx)_{\text{expected for } m_{TOF},\ z=1}}$$

Particle identification with the TOF & TPC

A cut on TPC signal within 2σ from the expected Bethe-Bloch value of the species under investigation is applied before fitting the TOF square mass distribution of light (anti-)nuclei.

$$\mu_{TOF}^2 = \left(\frac{m}{z}\right)_{TOF}^2 = \left(\frac{p}{z}\right)^2 \left[\left(\frac{t_{TOF}}{L}\right)^2 - \frac{1}{c^2}\right]$$

$$z_{TPC}^2 = \frac{(dE/dx)_{TPC}}{(dE/dx)_{\text{expected for } m_{TOF},\ z=1}}$$

A sample of about 10^6 anti-deuterons and 2000 $^3\overline{He}$ is selected by these cuts.

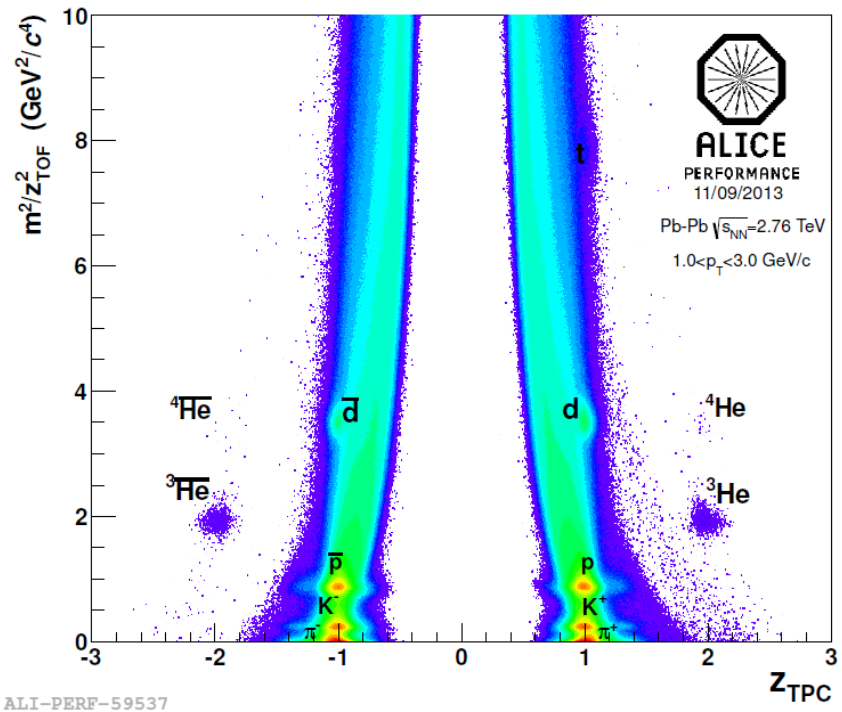

Secondaries rejection

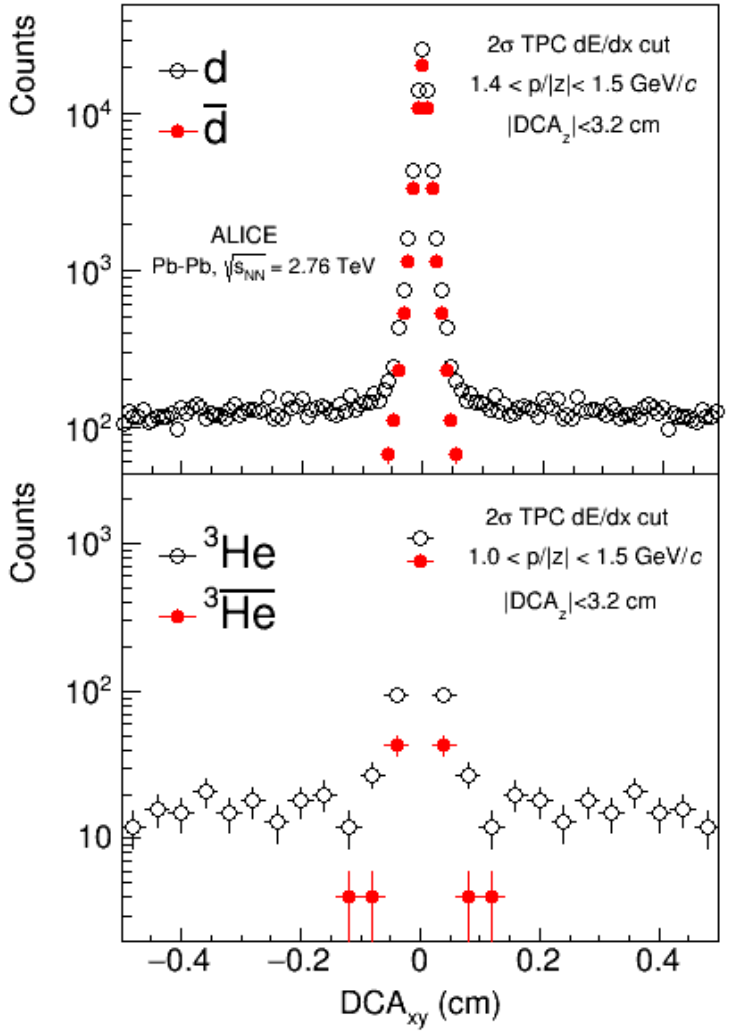

Secondaries from material (only for nuclei) can be biased because they don't come from the the primary vertex → wrong time-of-flight in the first millimeters.
A tight cut on DCA_{xy} was applied (< 1 mm) to reduce their influence.

Contamination from secondary nuclei reduced to a level below 3%.

Fit to square mass distribution

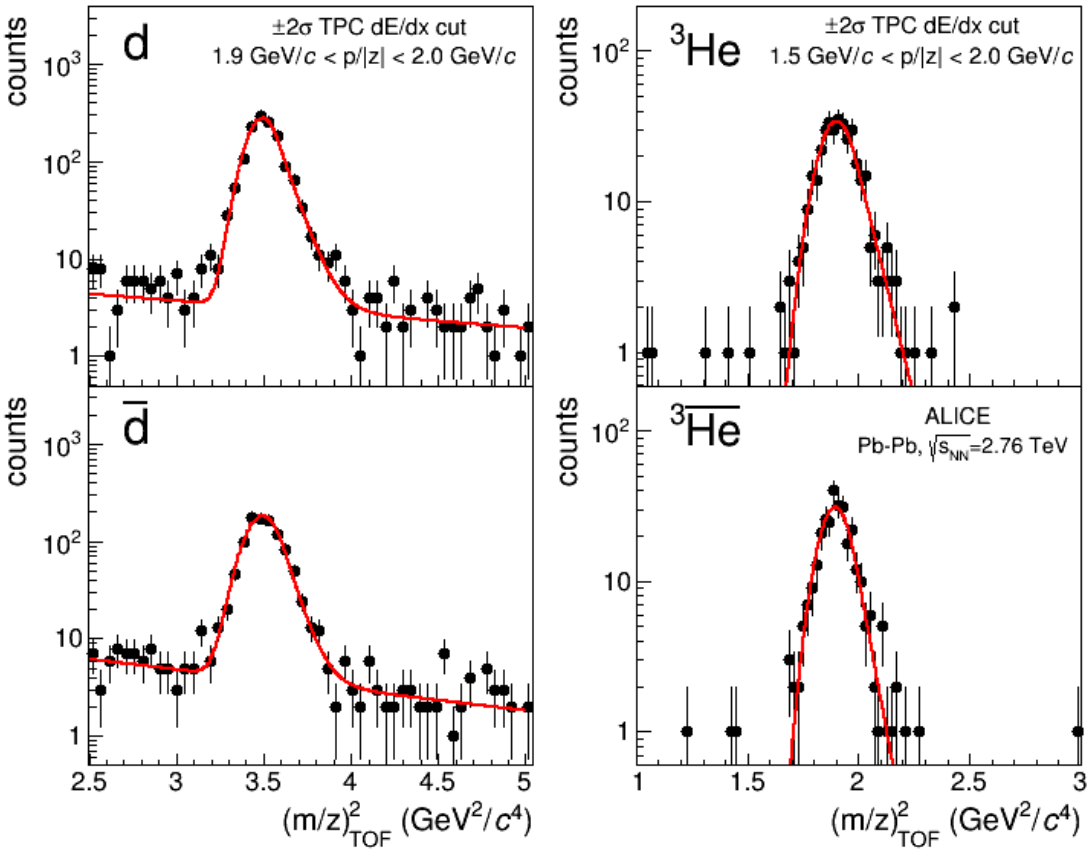

$$\mu^2_{TOF} = \left(\frac{m}{z}\right)^2_{TOF} = \left(\frac{p}{z}\right)^2 \left[\left(\frac{t_{TOF}}{L}\right)^2 - \frac{1}{c^2}\right]$$

Fits were performed in rigidity (*p/z*) and pseudorapidity intervals.

The **fit function** used has two terms: **signal** + **background**

Signal = **Gaussian** distribution **with a small exponential tail** on the right to describe the **TOF time response**.

Background = **Exponential distribution** to fit residual background (in the deuteron case only)

Correction with (anti)proton mass

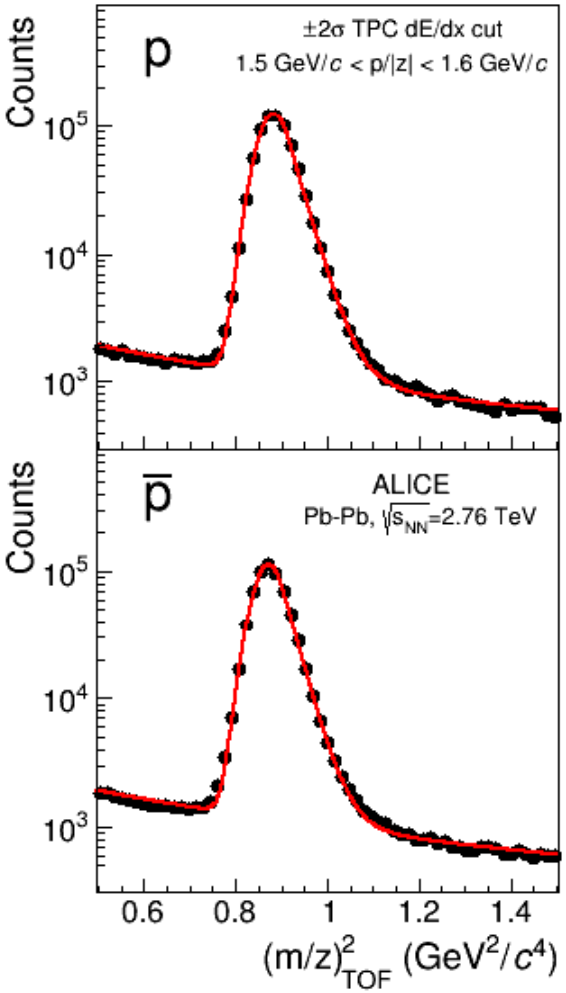

Protons and anti-protons mass distributions are fitted as well and used to correct for charge-dependent systematics assuming $m_p = m_{\bar{p}}$.

$$\mu_{A(\bar{A})} = \mu^{TOF}_{A(\bar{A})} \times \frac{\mu^{PDG}_{p(\bar{p})}}{\mu^{TOF}_{p(\bar{p})}}$$

This variable allows the cancellation of all the contributions which are mass independent.

TOF → measured values
PDG → values provided by the Particle Data Group

The magnetic field configurations

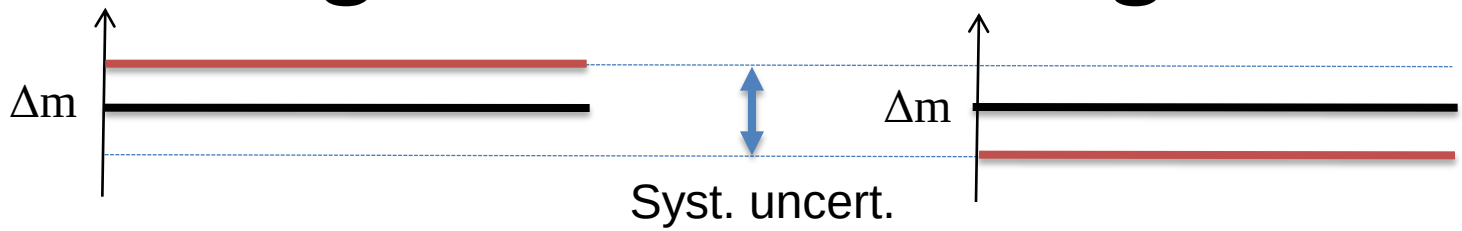

Upon inversion of the magnetic field the residual effects due to mis-alignments and mis-calibrations are inverted.
The average in the two configurations is taken as the final result and the difference is used to give a systematic uncertainty.

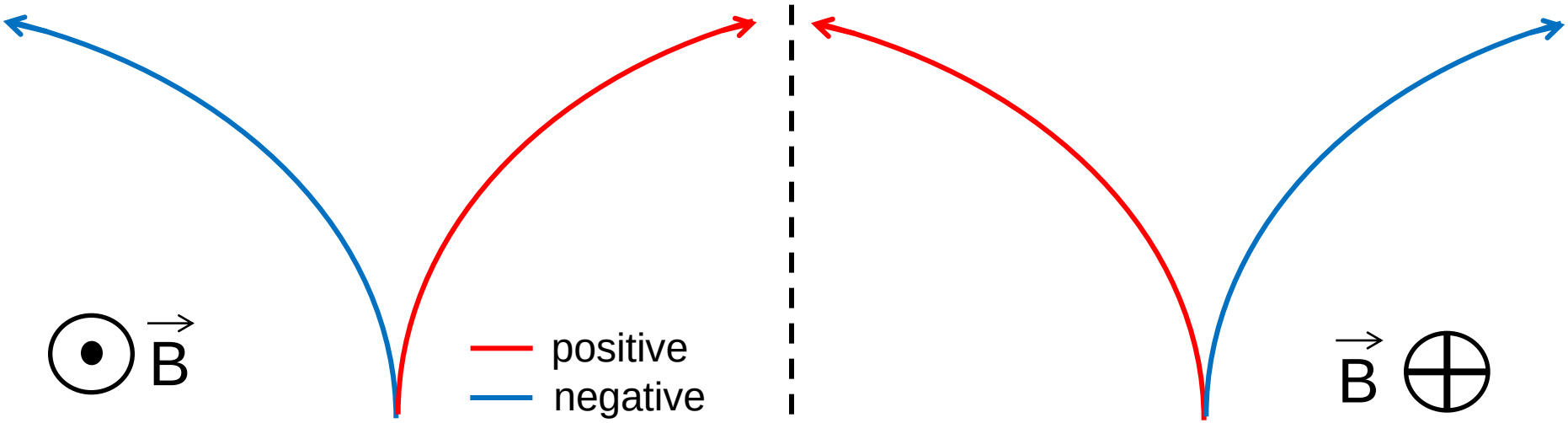

Other sources of systematic uncertainties

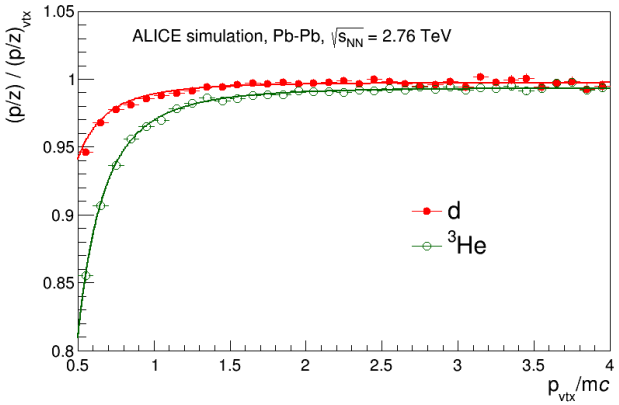

The rigidity entering the mass formula is a **mean rigidity**. Results with and without MC parameterization.

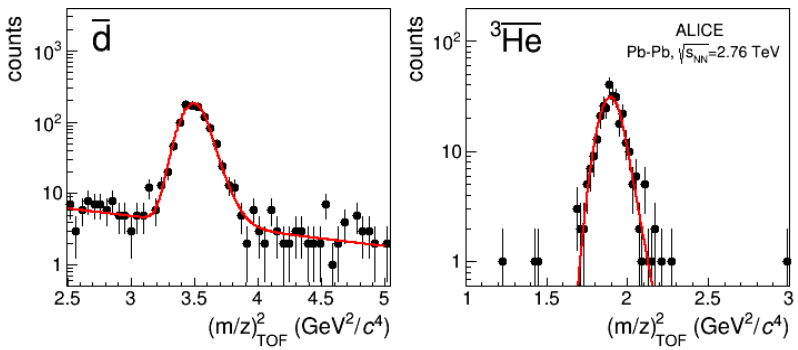

Fit procedure: the assumptions on the fit function and the range of the fit were varied.

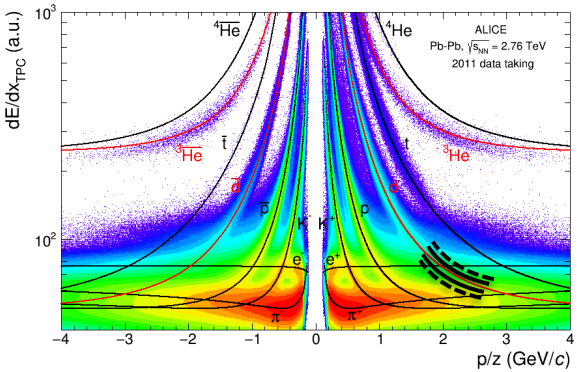

TPC dE/dx selection: other cuts (tighter or looser: from 1σ to 4σ) were tested.

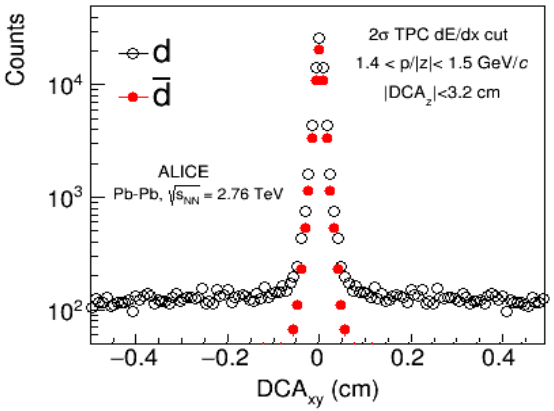

Sensitivity to the **DCA cuts**: a tight cut on the DCA_{xy} from the IP (<1 mm) is applied.

Summary of systematic uncertainties

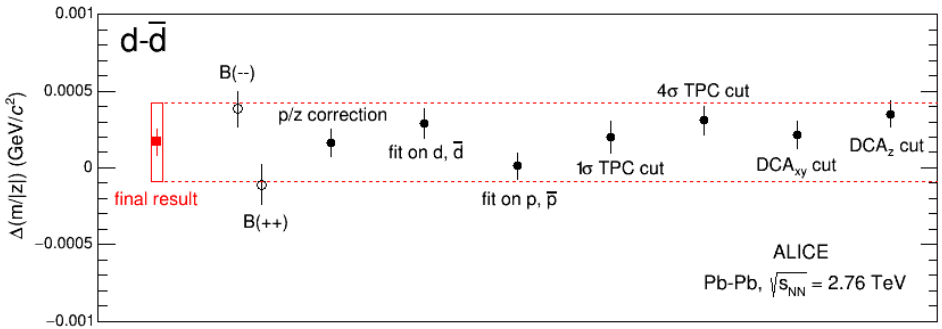

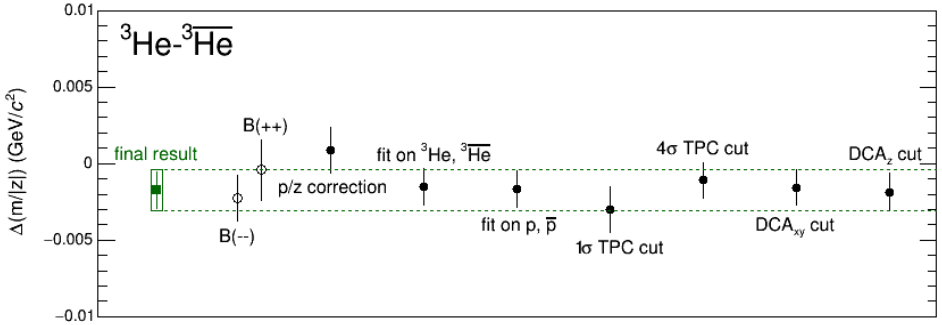

Systematic uncertainty	$\Delta\mu_{\mathrm{d\bar{d}}}/\mu_{\mathrm{d}}$ $(\times 10^{-4})$		$\Delta\mu_{^3\mathrm{He}^3\overline{\mathrm{He}}}/\mu_{^3\mathrm{He}}$ $(\times 10^{-3})$	
$p/\lvert z\rvert$	1.5 GeV/c	4.0 GeV/c	1.0 GeV/c	3.0 GeV/c
Tracking and alignment	± 0.7		negligible	
Mean rigidity correction	negligible		± 0.7	
Fit procedure	± 0.3	± 1	± 0.5	
TPC dE/dx selection	± 0.7		± 0.4	± 2.5
Secondaries	± 1	± 0.2	± 0.1	

The ALICE measurement

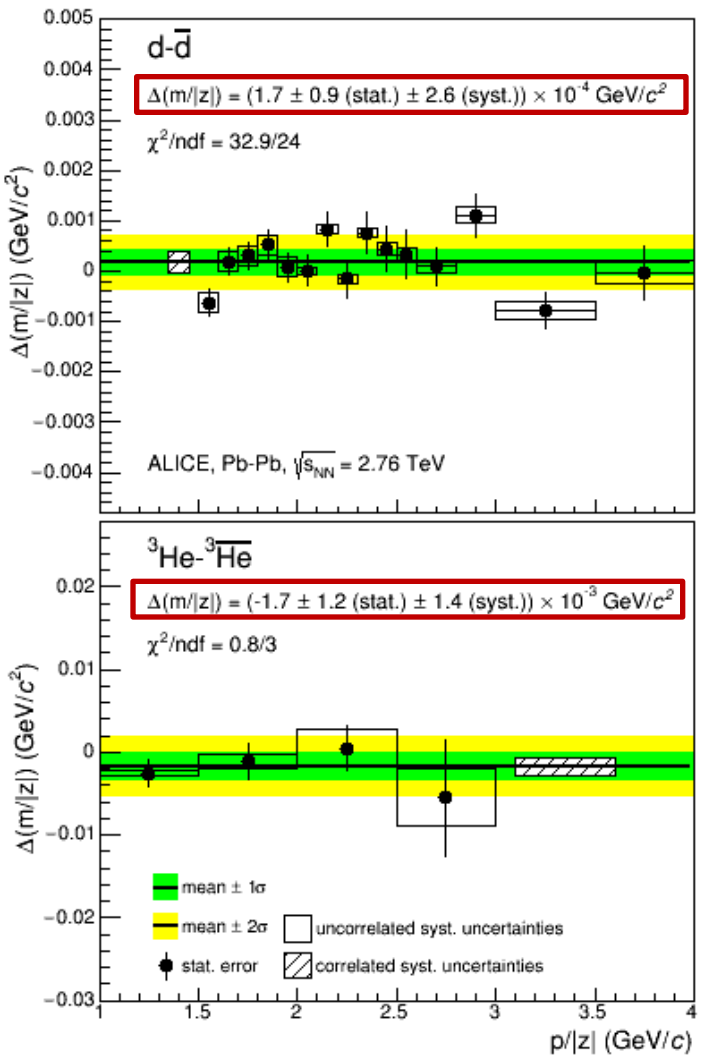

d-$\bar{d}$ (top) and ^{3}He-$^3\overline{\text{He}}$ (bottom) mass-over-charge ratio difference measurements as a function of the particle rigidity.

The **final measurement** is obtained from a weighted average over all rigidity bins.

Result: mass differences

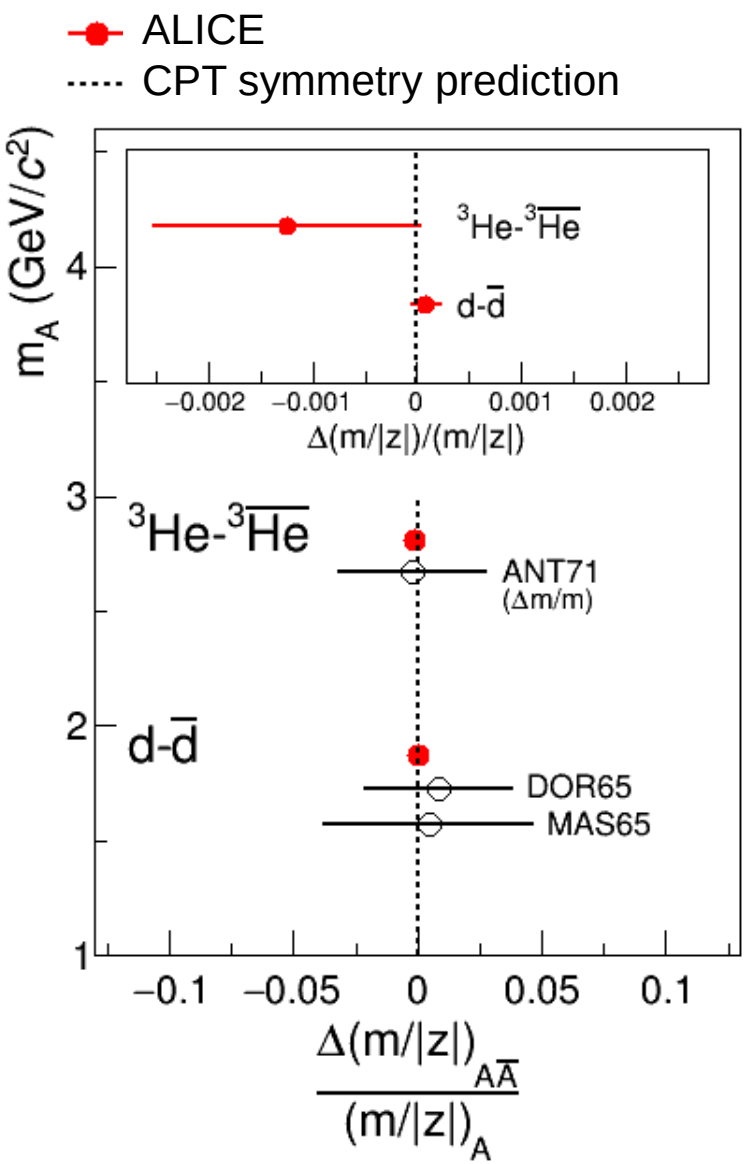

$$\frac{\Delta\mu}{\mu} = [0.9 \pm 0.5\ (\text{stat.}) \pm 1.4\ (\text{syst.})] \times 10^{-4} \qquad \mathbf{d\text{-}\bar{d}}$$

$$\frac{\Delta\mu}{\mu} = [-1.2 \pm 0.9\ (\text{stat.}) \pm 1.0\ (\text{syst.})] \times 10^{-3} \qquad \mathbf{^3He\text{-}\,^3\overline{He}}$$

Highest precision direct measurements of mass difference in the sector of nuclei

Improvement by one to two orders of magnitude compared to previous measurements obtained more than 40 years ago

ANT71: Nucl. Phys. B31 (1971) 235
DOR65: Phys.Rev.Lett 14 (1965) 1003
MAS65: Nuovo Cim. 39 (1965) 10

Result: binding energy differences

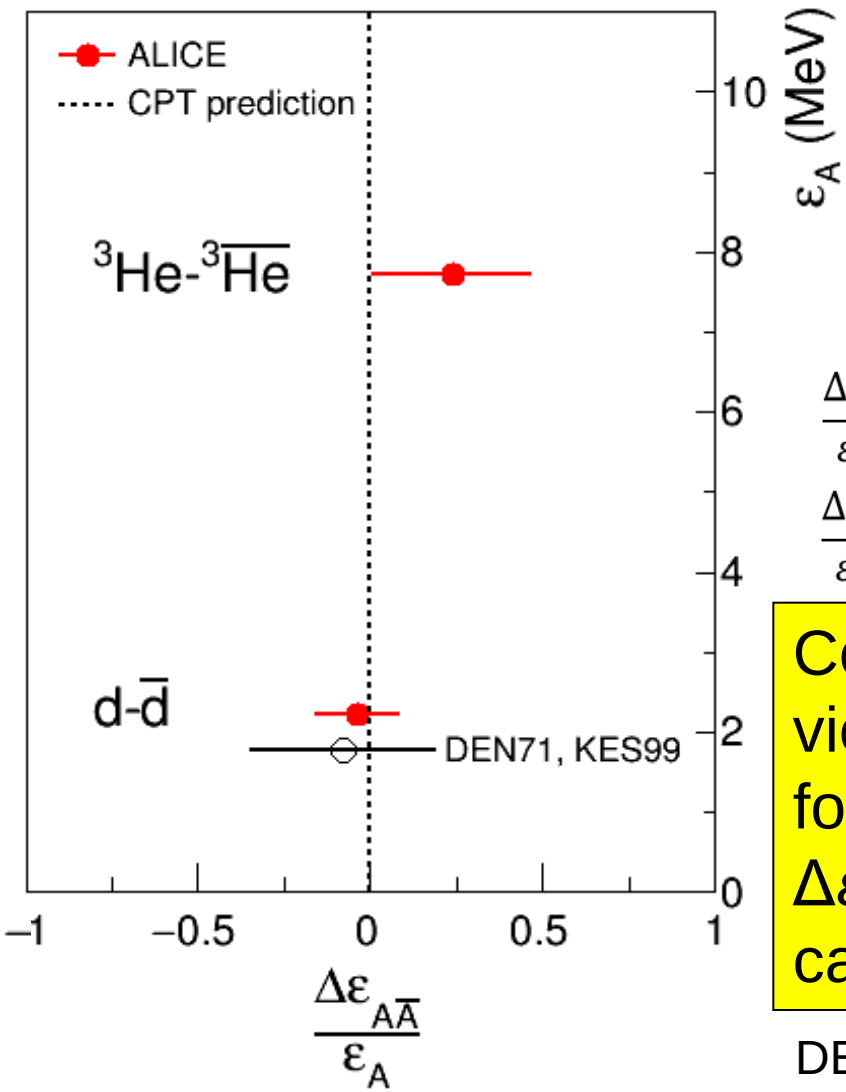

$$\Delta\varepsilon_{A\bar{A}} = Z\Delta m_{p\bar{p}} + (A-Z)\Delta m_{n\bar{n}} - \Delta m_{A\bar{A}}$$

$\Delta m_{p\bar{p}} < 7\times10^{-10}\,\text{GeV}/c^2 \quad (\text{CL} = 90\%)$

Nature, 574 (2011) 484

$\Delta m_{n\bar{n}} = (0.85 \pm 0.51(\text{stat.}) \pm 0.29(\text{syst.}))\times10^{-4}\,\text{GeV}/c^2$

Phys.Lett. B177 (1986) 206

$$\frac{\Delta\varepsilon}{\varepsilon} = -0.04 \pm 0.05\ (\text{stat.}) \pm 0.12\ (\text{syst.}) \qquad \mathbf{d\text{-}\bar{d}}$$

$$\frac{\Delta\varepsilon}{\varepsilon} = 0.24 \pm 0.16\ (\text{stat.}) \pm 0.18\ (\text{syst.}) \qquad \mathbf{^3He\text{-}^3\overline{He}}$$

Constraint on CPT symmetry violation improved **by a factor two** for (anti-)deuteron case.
$\Delta\varepsilon$ determined for the first time in case of (anti-)^{3}He.

DEN71: Nucl. Phys. B31 (1971) 253
KES99: Phys.Lett. A255 (1999) 221

CPT invariance tests

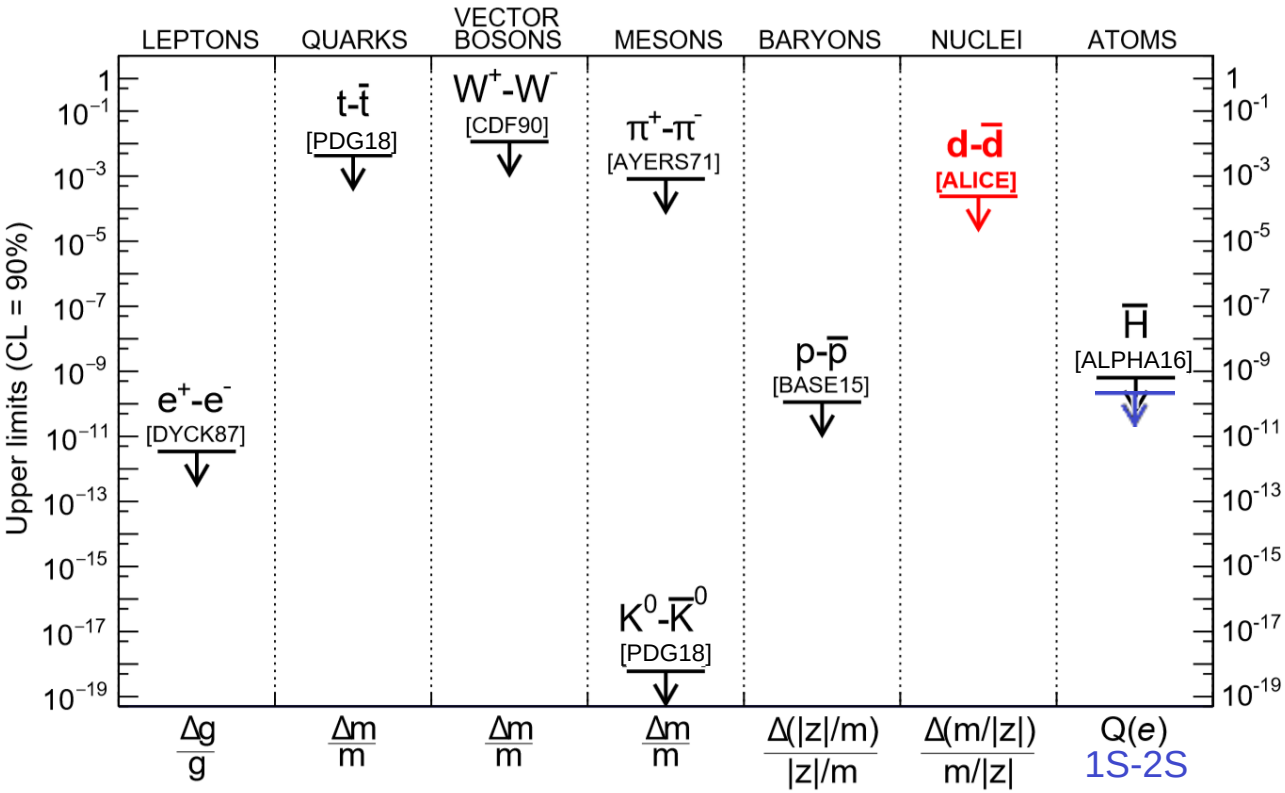

Experimental limits are also used to constrain, for different interactions, CPT violating terms added to the SM Lagrangian in the Standard Model Extension (SME)
(Rev. Mod. Phys. 83 (2011) 11)

ALICE-PUBLIC-2015-002
https://cds.cern.ch/record/2033777

Looking forward: Run 3+4

A very significant improvement of the int. luminosity expected for the Run 3+4 of LHC (2020-2028) + ALICE upgrade

(100 times more than RUN 1 i.e. $\mathcal{L}_{int}$=10 nb^{-1})

antideuteron and ^{3}He → RUN 1 statistics x 100÷1000

^{4}He → similar statistics as for ^{3}He at RUN 1 (but binding energy 4 times larger)

Table 3: Expected yields for light (hyper)nuclear states (and their antiparticles) for central Pb–Pb collisions (0–10%) at $\sqrt{s_{\rm NN}}$ = 5.5 TeV. From left to right: (hyper)nuclear species, production yield from the statistical hadronization model [396], branching ratio (only for hypernuclei and exotica states), rapidity interval, and number of expected reconstructed particles for $L_{\rm int}$ = 10 nb^{-1} [245] and reference for the estimation of the average acceptance-times-efficiency $\langle Acc. \times \epsilon \rangle$ for $p_{\rm T} > 0$.

State	dN/dy	B.R.	$\lvert y \rvert <$	Yield	Ref.
d (TPC)	5×10^{-2}	–	0.5	3.1×10^{8}	[388]
d (TPC+TOF)	5×10^{-2}	–	0.5	1.4×10^{8}	[388]
^{3}He (TOF)	3.5×10^{-4}	–	0.5	2.2×10^{6}	[388]
^{4}He (TPC+TOF)	7.0×10^{-7}	–	0.5	1.5×10^{3}	[388]
$^3_\Lambda$H	1.0×10^{-4}	0.25	1	4.4×10^{3}	[396]
$^4_\Lambda$H	2.0×10^{-7}	0.50	1	1.1×10^{2}	[396]
$^4_\Lambda$He	2.0×10^{-7}	0.54	1	1.3×10^{2}	[396]
Λn	3.0×10^{-2}	0.35	1	2.9×10^{7}	[397]
$\Lambda\Lambda$	5.0×10^{-3}	0.064	1	1.9×10^{5}	[397]
$\Lambda\Lambda$	5.0×10^{-3}	0.41	1	1.2×10^{6}	[397]

Frascati Phys.Ser. 62 (2016) arXiv:1602.04120

Conclusions

- The abundant production rate of (anti)nuclei in ultrarelativistic heavy-ion collisions combined with the unique **PID capability of the ALICE experiment** allows one to test the CPT invariance in nucleon-nucleon interactions.

- The measurements of the difference of the mass-over-charge ratio between d and $\bar{d}$, and ^{3}He and $^{3}\overline{\mathrm{He}}$ have been performed, improving by **one to two orders of magnitude** previous results obtained more than 40 years ago.

- The results are also expressed in terms of binding energy differences. The value obtained for the (anti-)deuteron case improves by a **factor two** the constraints inferred by existing measurements. In the case of (anti)^{3}He the binding energy difference has been determined for the first time, with a precision comparable to the (anti-)deuteron case.

- Remarkably, these improvements are reached in an experiment which is not specifically dedicated to CPT test and which will continue to take data in the next years, with an expected **increase in luminosity up to a factor 100**.

ALICE

Thank you for your attention!

Backup

Tracking performance and track selection

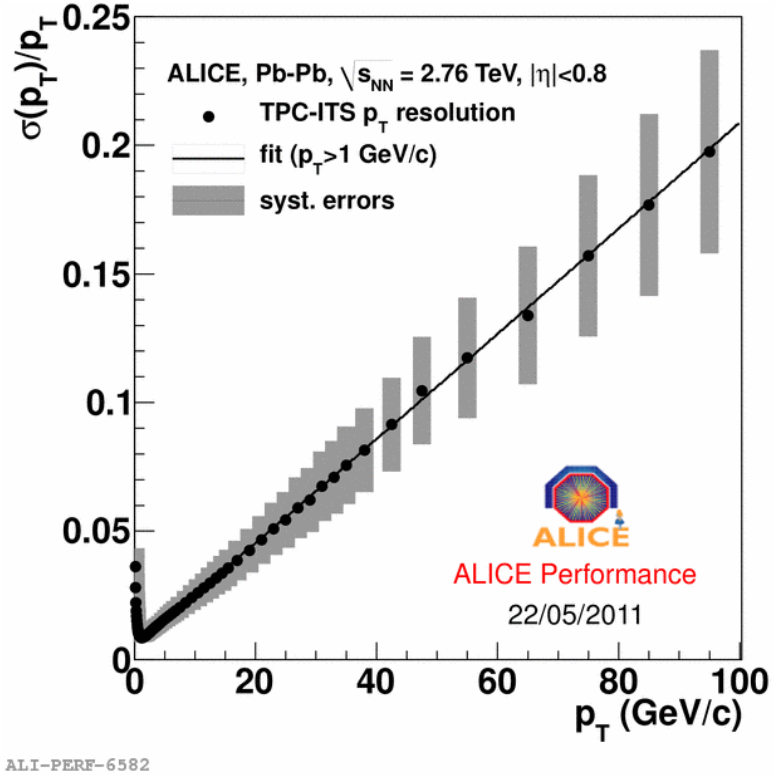

Int. J. Mod. Phys. A 29 (2014) 1430044

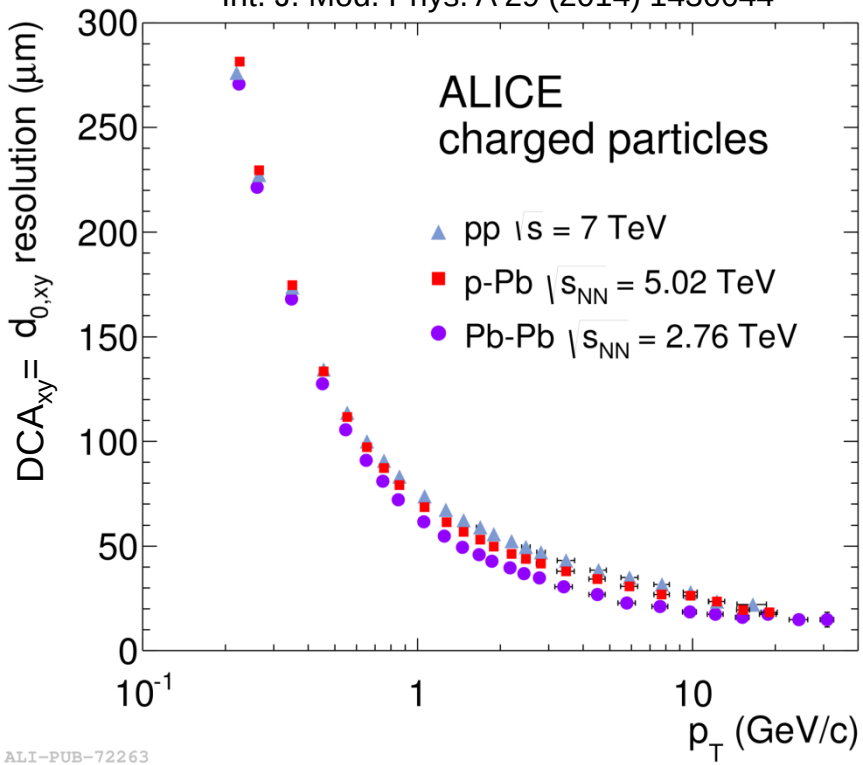

Tracks are selected requiring ITS-TPC standard cuts and a TOF time signal associated to the track.

Additional cuts on the distance of closest approach (DCA) from the IP are applied to reject secondary particles

Charge-dependent systematics

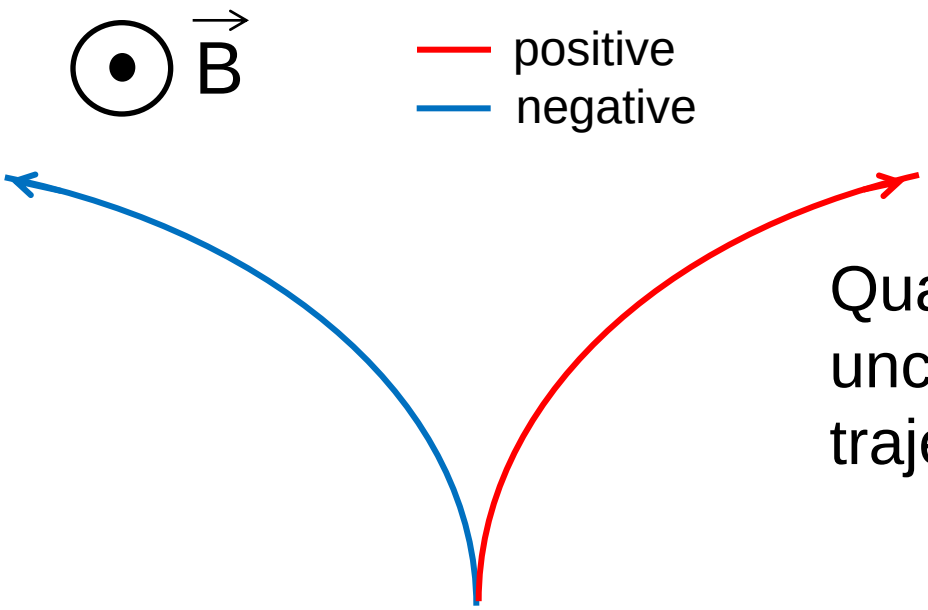

$$\mu_{TOF}^2 = \left(\frac{m}{z}\right)_{TOF}^2 = \left(\frac{p}{z}\right)^2 \left[\left(\frac{t_{TOF}}{L}\right)^2 - \frac{1}{c^2}\right]$$

Quantities sensitive to different uncertainties because of different trajectories.

Two ways to keep these systematics under control:

1. The main effect is mass independent and can be corrected for proton (+) and anti-proton (-) masses used as a reference.
2. The residual uncertainties can be estimated inverting the magnetic field (swapping positive/negative trajectories)

Mean rigidity parameterization

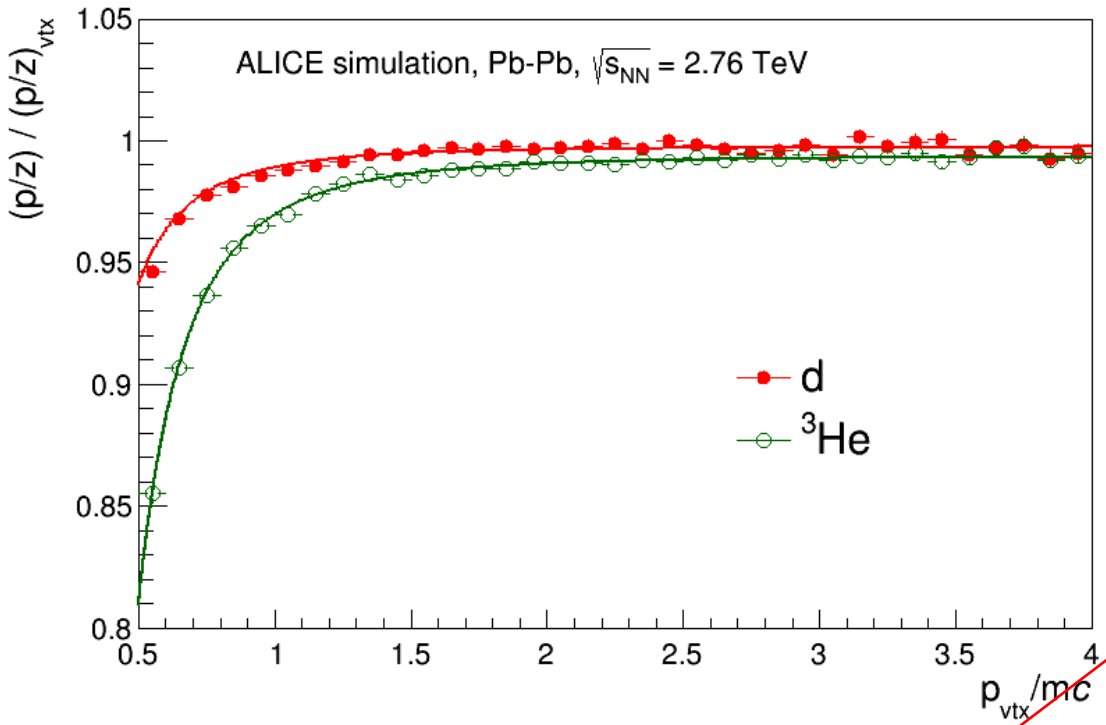

Due to energy loss the measured mass depends on the mean rigidity.
A MC parameterization was used to derive mean rigidity from the one measured at the interaction point .

$$\mu_{TOF}^2 = \left(\frac{m}{z}\right)_{TOF}^2 = \left(\frac{\langle p \rangle}{z}\right)^2 \left[\left(\frac{t_{TOF}}{L}\right)^2 - \frac{1}{c^2}\right]$$

On the correction based on (anti-)proton mass

$$\mu_{TOF}^2 = \left(\frac{m}{z}\right)_{TOF}^2 = \left(\frac{p}{z}\right)^2 \left[\left(\frac{t_{TOF}}{L}\right)^2 - \frac{1}{c^2}\right]$$

$$\frac{1}{\mu}\frac{\partial \mu}{\partial p} = \frac{1}{p}$$

$$\frac{1}{\mu}\frac{\partial \mu}{\partial L} = \frac{1}{L}\gamma^2$$

$$\frac{\Delta \mu}{\mu} = \frac{\Delta p}{p}$$

$$\frac{\Delta \mu}{\mu} = \frac{\Delta L}{L}\gamma^2$$

+ *L*-*p* correlation term

$$\frac{\Delta \mu}{\mu} = 0$$

$$\frac{\Delta \mu}{\mu} = \frac{\Delta L}{L}\left(\gamma_{A(\bar{A})}^2 - \gamma_{p(\bar{p})}^2\right)$$

$$\mu_{A(\bar{A})} = \mu_{A(\bar{A})}^{TOF} \times \frac{\mu_{p(\bar{p})}^{PDG}}{\mu_{p(\bar{p})}^{TOF}}$$

The Start Time (t_{ev}) provided by TOF

Int. J. Mod. Phys. A 29 (2014) 1430044

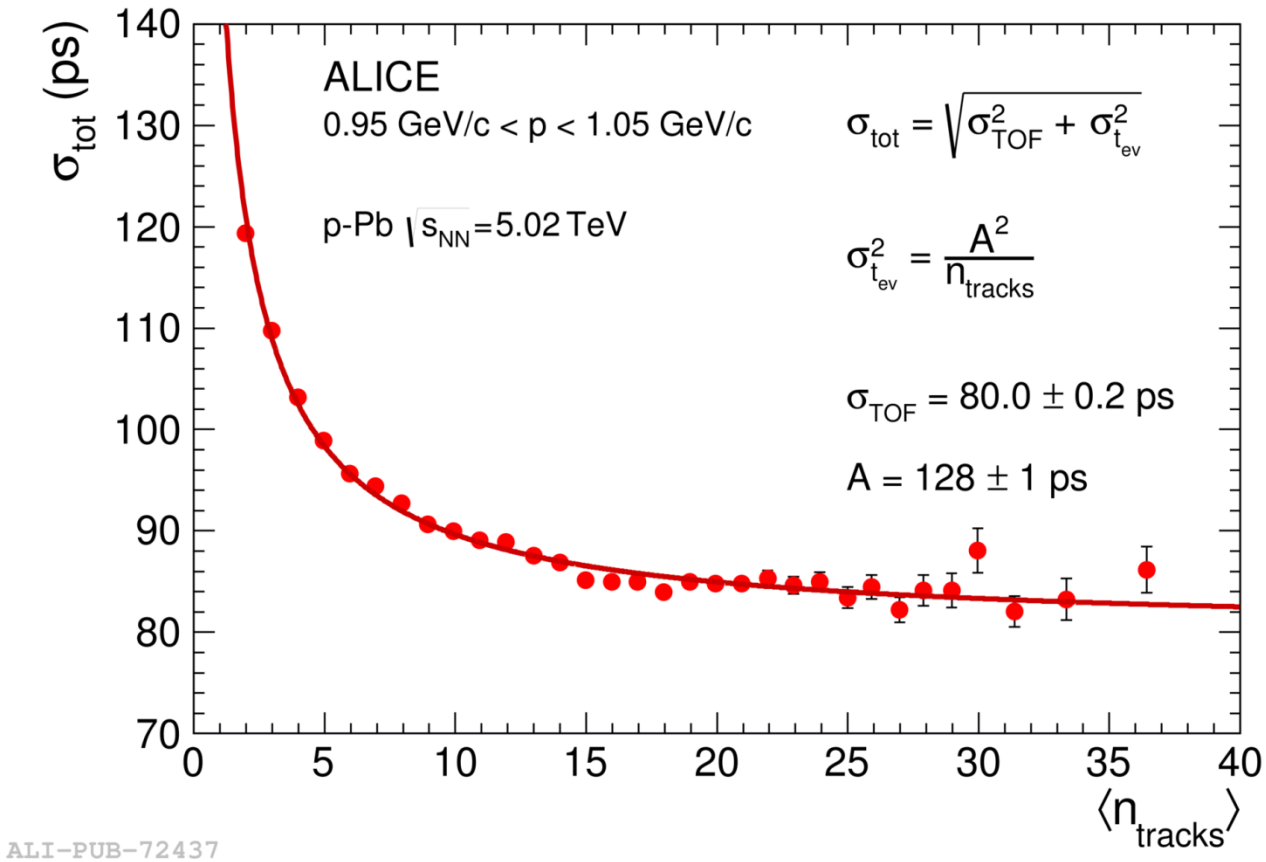

In Pb-Pb collisions the start time is provided by TOF, while in p-p collisions the TZERO detector is also used.